

Photometric Properties of Retroreflective Materials in Dependence on their Structure and Angle of Illumination

DOI: 10.5604/01.3001.0013.0743

Central Institute for Labour Protection
– National Research Institute
Czerniakowska 16 00-701 Warsaw
* e-mail: jmszkudlarek@poczta.onet.pl

Abstract

The purpose of high visibility products is to reflect light at a low angle towards the source, such as vehicle headlights. The article presents measurements of the photometric properties of selected retroreflective materials made either of microlenses on a textile base or microprisms on a polymer base. The effects of the structure of the textile and polymer layers on the photometric properties of high visibility materials is analysed and the test methods applied are described.

Key words: retroreflective properties, retroreflective materials, high visibility products, microprism structures, microlens structures.

Introduction

According to statistics of the Police Headquarters, as many as 3.026 people died in road traffic accidents in Poland in 2017. Pedestrian collisions with vehicles were the second most common cause of accidents, with 7.911 such events recorded in that year. As a result, 861 people died and 7.473 were injured [1]. The underlying causes of such a high accident rate are the poor visibility of pedestrians and a lack of care both on the part of pedestrians and drivers. The obligation to use reflective elements by pedestrians moving along roads outside built-up ar-

reas (residential zones) was adopted to improve their visibility [2]. This measure contributed to a decrease in the number of accidents and fatalities by 170 and 51, respectively, relative to 2015. Despite a downward trend in accidents after the law came into force, the number of fatalities and injuries still remains very high. Among the many contributing factors, special attention should be paid to the limited effectiveness of reflective products due to directional light reflection and the large number of unsafe reflective products available on the market. An audit carried out in 2015 by the Polish Office of Competition and Consum-

er Protection [3] showed that over 90% of the commercially available reflective products investigated did not meet the essential requirements of the Personal Protective Equipment Regulation 2016/425.

Reflective products are made using two alternative technologies [4, 5], which differ in terms of the structure of reflective elements. One technology uses microlenses attached to a base fabric with a silver-plated adhesive layer to form a mirror-like surface. The retroreflective effectiveness of such materials depends on the geometry of the lenses as well as on their arrangement and depth of embedment. The durability of microlens tapes depends on the adhesive properties of the components, the flexibility of the adhesive layer, and on the strength of the base fabric.

The other technology uses microprisms attached to reflective polymer materials. Such materials consist of multilayer polymeric structures, with the middle layer exhibiting a relief in the shape of vertices of geometrical figures made of a synthetic filler resin, whose base is a thin carrier film. The optical properties of these materials depend on their layered structure and microprism shape and aggregation (arrangement) [6-9]. A diagram showing the structure of materials with reflective properties is given in **Figure 1**.

High visibility materials produced using the technologies described above are applicable in two different areas. Reflective textile products are sewn onto high visibility protective clothing and accessories for professional and non-professional use. In turn, reflective polymeric materials (foils) are used mainly in the auto-

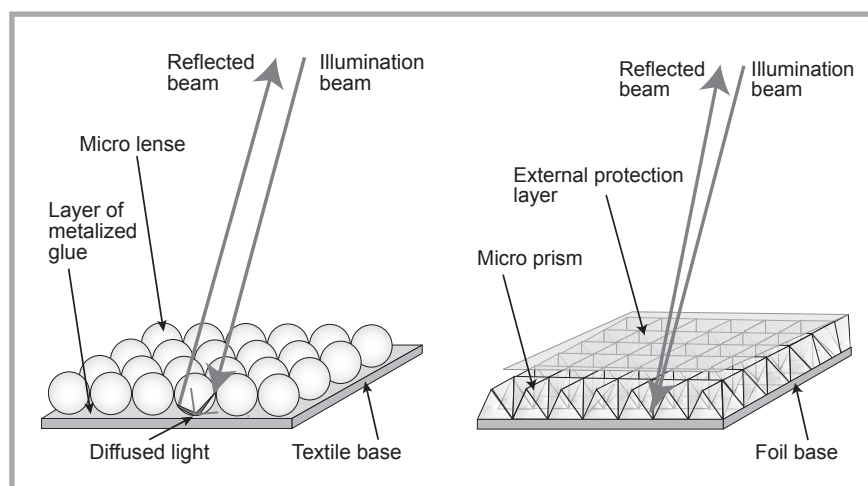


Figure 1. Structure of reflective materials: a) with microlenses, b) with microprisms.

Table 1. Retroreflective microprism and microlens materials selected for tests.

Sample no.	Description
1.	Textile tape for sewing on fabrics with a microlens surface; 100% polyester; grey color; average diameter of microlenses 65,4 μm [11]
2.	Textile tape for sewing on fabrics with a microlens surface; 100% polyester; grey color; average diameter of microlenses 42,6 μm [11]
3.	High gloss microprismatic polypropylene film; red colour
4.	High gloss microprismatic polypropylene film; grey colour

motive industry and in road engineering to mark surfaces off against a specific background.

The available data show that materials containing microprisms have a higher surface density of the reflectance factor within a low angle with respect to incident light. As a result, they are visible from a greater distance (vs. microlens materials) when illuminated by the light of an oncoming vehicle perpendicular to the surface of the retroreflector. Another advantage is a smaller loss of reflective properties of the material due to precipitation. On the other hand, reflective materials containing microlenses provide better visibility at angles other than perpendicular to the direction of incident light beams due to greater dispersion of reflected light [4].

The aim of the study presented is to assess the influence of structural characteristics of reflective materials produced using two technologies (microlenses and microprisms) on their photometric properties evaluated in accordance with the requirements described in the harmonised standard [10].

Materials

Commercially available high visibility materials (highly reflective textile straps and sheets) containing microspheres and microprisms on a textile base or microprisms on the surface of polymer films were tested (see *Table 1*).

Samples 1 and 2 were grey 50 mm wide textile tapes, sample 3 – a red polymer film with a size of 200 mm × 200 mm, and sample 4 was a grey polymer film with

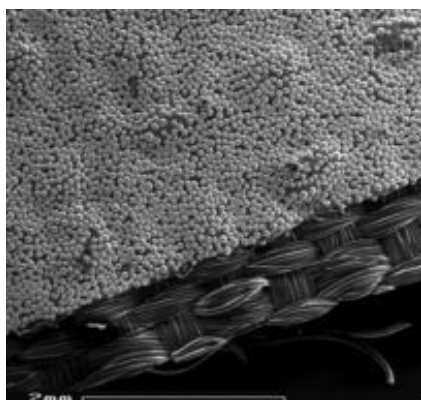


Figure 3. Structure of retroreflective fabric produced using microlens technology <http://www.foton.if.uj.edu.pl/document-s/12579485/7074ffff-6bd1-4472-88e6-8e-1a848b9a6b> [15].

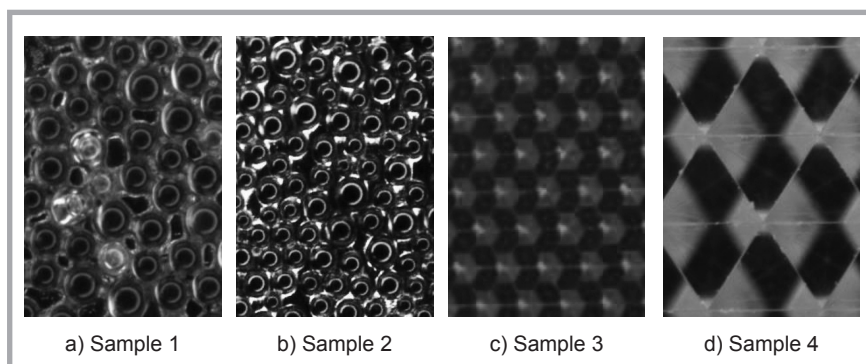


Figure 2. Structure of the reflective materials studied, commonly used to improve the visibility of people and objects.

a size of 150 mm × 150 mm. The samples were examined using an Opta-Tech (Poland) microscope equipped with a 2 MP digital camera of a real surface area of 0.72 × 1.19 mm (320 × 456 px). The images acquired are shown in *Figure 2*.

Analysis of the surface structure of the reflective materials tested reveals that microlens samples 1 and 2 have an irregular and inhomogeneous structure of reflective elements, with visible free spaces and spaces filled with adhesive resin. The microlenses differ in diameter and are attached to a base textile

material (woven fabric) characterised by a heterogeneous spatial architecture of the surface (mainly resulting from yarn characteristics, weave type, warp and weft density, and structural phases of the fabric [12-14]). Due to the inhomogeneity of the substrate surface observed, the microlenses are arranged in an irregular way (see *Figure 3*).

This study involved retroreflective woven tapes. A Delta Optical Smart 2 MP digital microscope was used to acquire microphotographs of structures with dimensions of 7 mm × 5.25 mm (640 × 480 px)

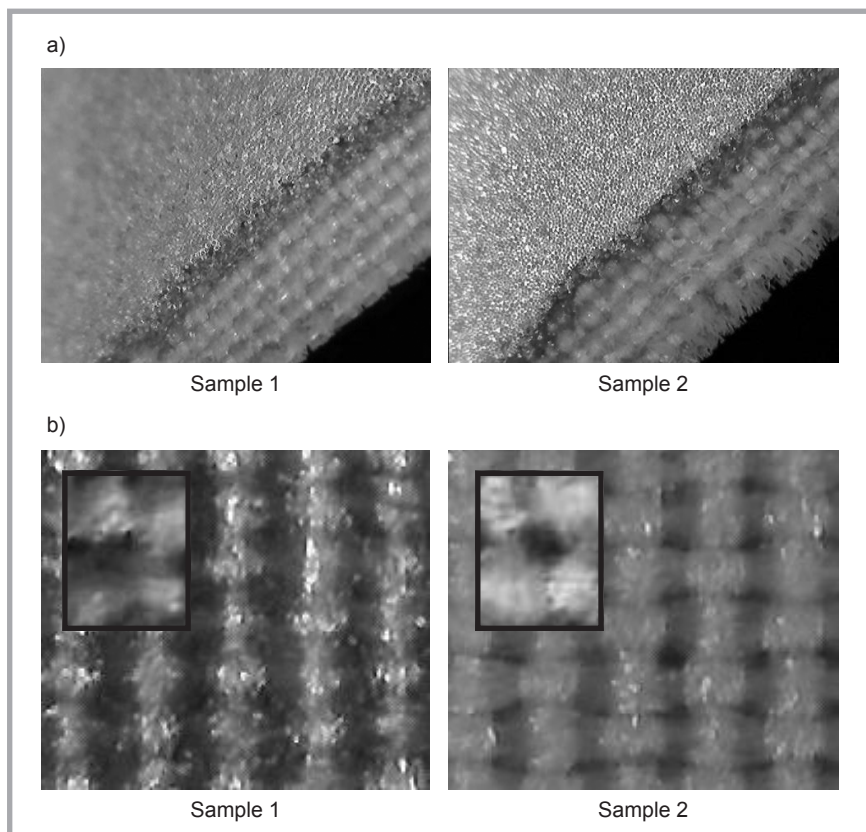


Figure 4. Structure of woven retroreflective materials: a) cross-section of reflective tape, b) weave structure of 2.07 mm × 1.80 mm size (189 × 165 px) with an SMS 1 structure module (64 × 51 px with a size of 0.70 mm × 0.56 mm).

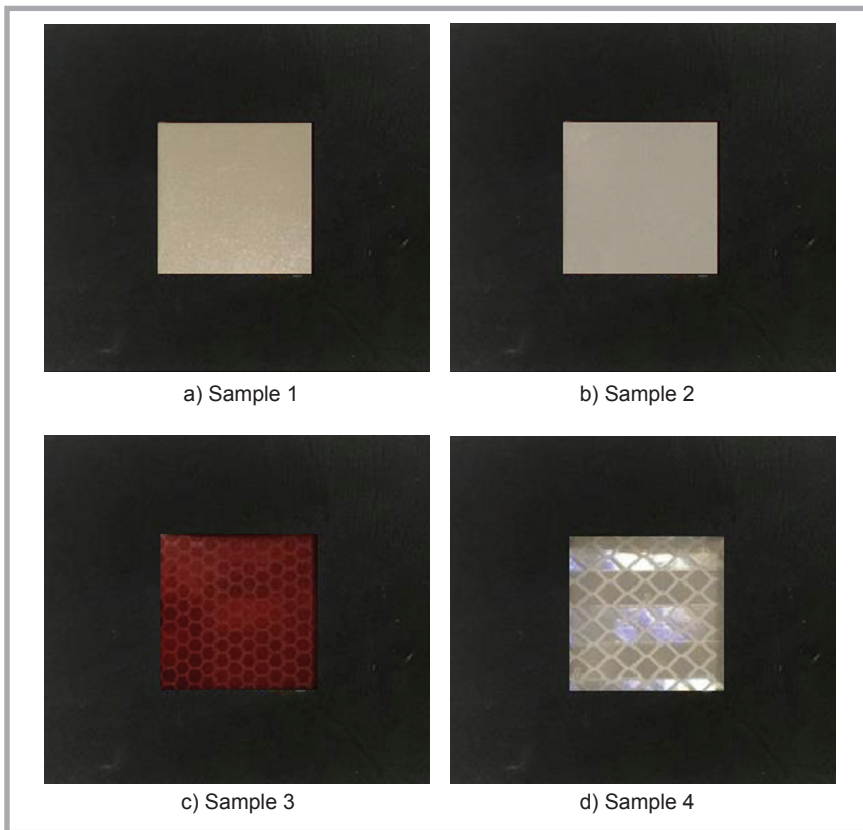


Figure 5. Photographs of samples prepared for tests.

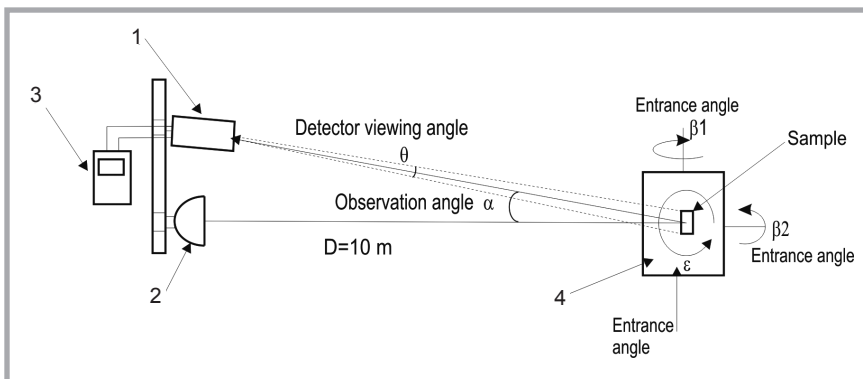


Figure 6. Schematic diagram of the photometric set-up for testing high visibility materials: 1) detector; 2) illuminator; 3) photometer; and 4) goniometer.

and weave structures with dimensions of $2.07 \text{ mm} \times 1.80 \text{ mm}$ ($189 \times 165 \text{ px}$), with SMS 1 structural modules ($64 \times 51 \text{ px}$). The woven retroreflective tapes are shown in **Figure 4**.

Reflective tape 1 has the same structural parameters as tape 2, as can be seen from the images in **Figure 4.b**. The fabric structure of sample 1 is disturbed by a layer of resin which migrated deeper into it. However, the type of weave is still recognisable – in both materials it is a plain weave with a warp and weft density of 7 and 12 threads per cm, respectively.

The process of application of microlenses on a base material is to the greatest extent affected by the adhesive properties of the components and the occurrence of varying stresses in the fabric during the deposition of the reflective layer.

In addition, as can be seen from **Figure 3**, the microlenses follow the fabric structure, and particularly the relief characteristic of the weave. This causes an inhomogeneous arrangement of the reflective elements, leading to some light scattering, which affects retroreflection [15, 16].

In the case of materials made using micropism technology, the surface material is characterised by a highly regular orientation of reflective elements (see **Figure 2.c, 2.d**). The uniformity and regularity of the light reflecting elements is important and directly translates into their photometric properties. Such materials, particularly in the form of self-adhesive reflective polymer films, are widely used in sectors with high economic potential, including the automotive industry and road construction [17-19]. They are commonly used to improve the visibility of road signs and barriers, as well as vehicle and road markings. However, in practice, textile-based materials are characterised by a higher retroreflective coefficient at low angles (up to 0.33°) as compared to retroreflective micropism materials, due to technological limitations. In summary, the uniformity and regularity of light reflecting elements is crucial and directly affects the photometric properties of reflective materials.

Since road signs are immobile, they do not need to exhibit a wide viewing angle, and hence they should be preferably made of materials containing micropisms. On the other hand, pedestrians should be visible from the widest possible angle; therefore, in this case high visibility materials with microlenses are more suitable. It should be emphasised that the health and life of people in workplaces and in everyday situations depend on the quality of reflective materials and, in particular, retroreflective textile materials applied on clothing to improve the wearer's visibility. Therefore the technology of production of retroreflective microlens materials should be further improved.

After acclimatisation according to the standard method [10], the samples tested were mounted in $40 \text{ mm} \times 40 \text{ mm}$ frames (**Figure 5**).

A schematic diagram of the photometric set-up used for measurement of high visibility materials is shown in **Figure 6**. The setup was designed in accordance with Standard CIE 54 [20], consisting of the following:

- a goniometer,
- a system for orienting the illuminator and photometer head,
- an illuminator (halogen lamp and collimator),
- a detector for measuring luminance,

- a detector for measuring illuminance on the surface of the sample.

Photographs of the components of the photometric set-up used for testing are presented in **Figure 7**.

The detector head and positioning system could be set to observation angles of 0.2° , 0.33° , 1° and 1.5° by means of a handle (see **Figure 7**). The system enabled the detector to tilt depending on the measurement geometry. The illuminator consisted of a halogen lamp emitting a spectrum compliant with CIE illuminant A, equipped with an optical collimator. The diameter of the measuring beam on the goniometer gauge was 82 mm, which corresponds to approx. 28 minutes of arc for a measurement distance of $L = 10$ m. An HD2102.1 photo-radiometer with an LP 47 LUM 2 probe (DELTA OHM, Italy) was used for luminance measurements. The spectral sensitivity of the LP 471 LUM probe was consistent with the photopic vision curve with an accuracy of 92%. The detector viewing angle was 2° . An L-20A photometer (Sonopan, Poland) was used to determine the light intensity of the samples. The photometer was equipped with a silicon photodiode with a measurement range of 1 lx to 1,900 lx, with a resolution of 1 lx.

■ Experimental methods

The tests were conducted at an ambient temperature of $20\text{--}22^\circ\text{C}$ and relative humidity of $55 \pm 5\%$. The photometric properties of reflective materials were tested according to the method described in CIE 54 [20]. The coefficient of luminous intensity R' was obtained by comparing the light flux I (in candelas) reflected off

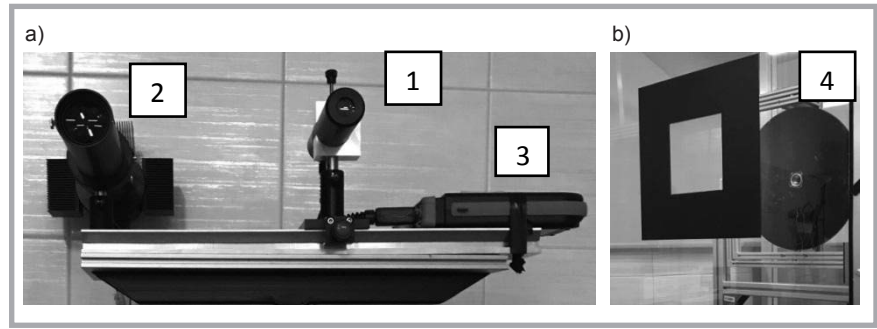


Figure 7. Components of the set-up used for determining the coefficient of luminous intensity R' : 1) detector 2) illuminator, 3) photometer and 4) goniometer.

a planar retroreflective sample, reaching the detector at specific observation and illumination angles, with the illuminance of sample E (in luxes) and the area of the retroreflector.

Measurements were carried out in a dark-room. A laser beam was used to adjust the height and parallel orientation of the illuminator, detector head, and goniometer. A DLE 70 laser rangefinder (Bosch, Germany) was used to measure the detector and illuminator distance from the sample (10.02 ± 0.007 m). The illuminance uniformity of the light beam incidence on the sample was measured using an L-20A photometer. Illuminance E values were measured at the center and around the circumference of the beam, which was 60 mm in diameter. The beam illuminating the sample was found to be homogeneous at $423 \text{ lx} \pm 1 \text{ lx}$.

Rectangular samples mounted in frames were attached to goniometer measuring disc using two-sided adhesive tape. Then luminance L was determined for the selected observation angle α and illumination angle β_1 [10]. The coefficient of

luminous intensity was calculated using **Equation (1)**.

$$R' = \frac{I/E}{A}, \text{ cd}\cdot\text{lx}^{-1} \text{ m}^2 \quad (1)$$

where:

- R' – coefficient of luminous intensity,
- I – luminous intensity, cd,
- E – illuminance, lx,
- A – illuminated sample area, m^2 .

The luminous intensity on the detector's surface I was calculated using **Equation (2)**:

$$I = L \cdot \pi (D \cdot \text{tg}(\theta/2))^2 \quad (2)$$

- L – luminance, cd/m^2 ,
- D – distance of the sample from the luminance detector, m,
- θ – viewing angle of the luminance detector, degrees.

■ Results and discussion

Values of the coefficient of luminous intensity determined for retroreflective microlens and microprism samples at different observation and illumination (entrance) angles are presented in **Figures 8-11**.

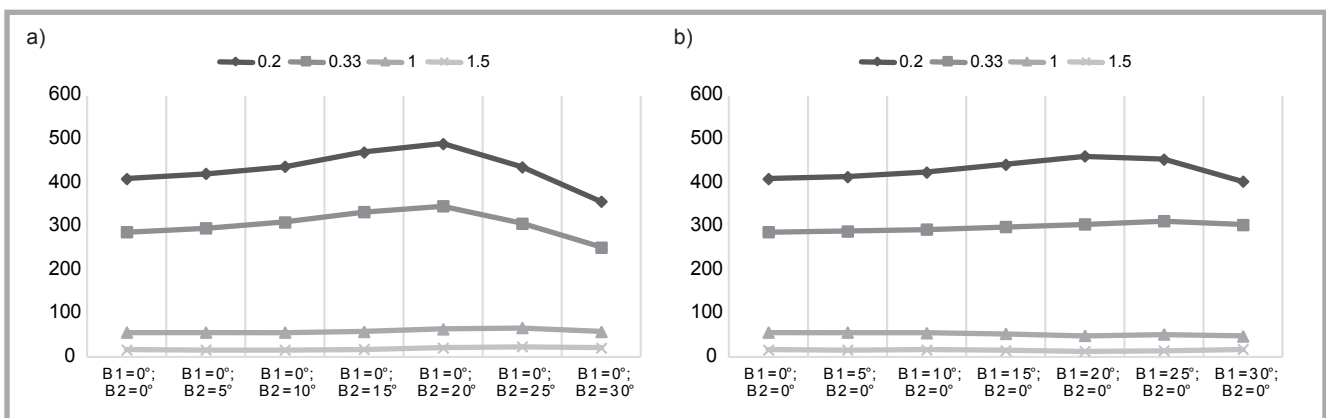


Figure 8. Coefficients of luminous intensity R' for sample 1 at observation angle α (0.2° , 0.33° , 1° , 1.5°) and at illumination angles β_1 and β_2 : a) $\beta_1 = 0^\circ$ and $\beta_2 = 0^\circ$, $\beta_2 = 5^\circ$, $\beta_2 = 10^\circ$, $\beta_2 = 15^\circ$, $\beta_2 = 10^\circ$, $\beta_2 = 20^\circ$, $\beta_2 = 30^\circ$; b) $\beta_2 = 0^\circ$ and $\beta_1 = 0^\circ$, $\beta_1 = 5^\circ$, $\beta_1 = 10^\circ$, $\beta_1 = 15^\circ$, $\beta_1 = 10^\circ$, $\beta_1 = 20^\circ$, $\beta_1 = 30^\circ$.

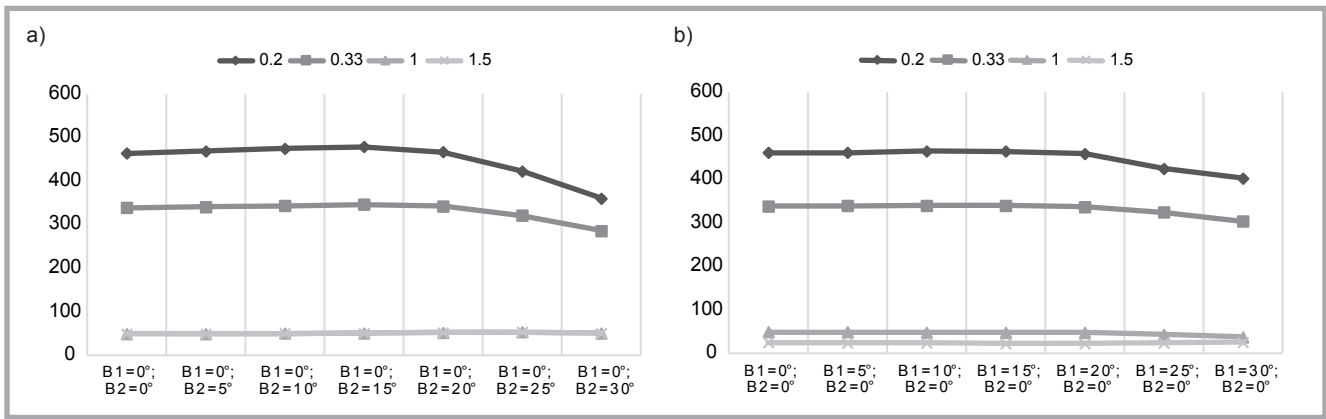


Figure 9. Coefficients of luminous intensity R' for sample 2 at observation angle α (0.2° , 0.33° , 1° , 1.5°) and illumination angles β_1 and β_2 : a): $\beta_1 = 0^\circ$ and $\beta_2 = 0^\circ$, $\beta_2 = 5^\circ$, $\beta_2 = 10^\circ$, $\beta_2 = 15^\circ$, $\beta_2 = 10^\circ$, $\beta_2 = 20^\circ$, $\beta_2 = 30^\circ$; b): $\beta_2 = 0^\circ$ and $\beta_1 = 0^\circ$, $\beta_1 = 5^\circ$, $\beta_1 = 10^\circ$, $\beta_1 = 15^\circ$, $\beta_1 = 10^\circ$, $\beta_1 = 20^\circ$, $\beta_1 = 30^\circ$.

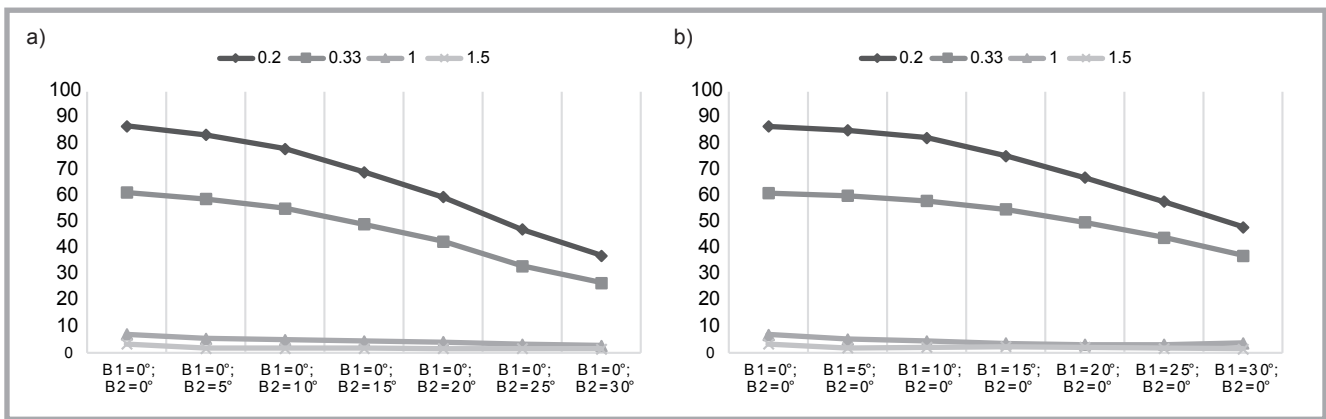


Figure 10. Coefficients of luminous intensity R' for sample 3 at observation angle α (0.2° , 0.33° , 1° , 1.5°) and illumination angles β_1 and β_2 : a): $\beta_1 = 0^\circ$ and $\beta_2 = 0^\circ$, $\beta_2 = 5^\circ$, $\beta_2 = 10^\circ$, $\beta_2 = 15^\circ$, $\beta_2 = 10^\circ$, $\beta_2 = 20^\circ$, $\beta_2 = 30^\circ$; b): $\beta_2 = 0^\circ$ and $\beta_1 = 0^\circ$, $\beta_1 = 5^\circ$, $\beta_1 = 10^\circ$, $\beta_1 = 15^\circ$, $\beta_1 = 10^\circ$, $\beta_1 = 20^\circ$, $\beta_1 = 30^\circ$.

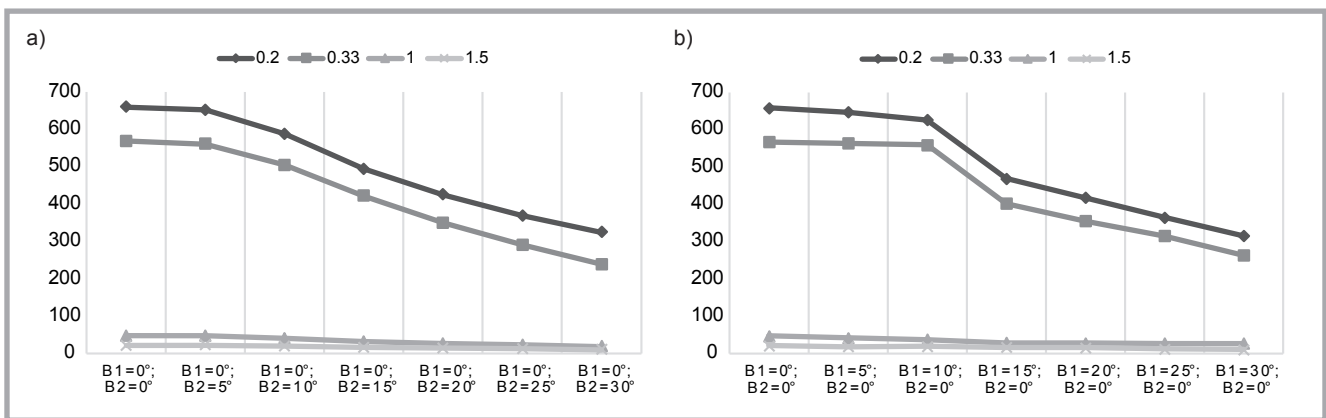


Figure 11. Coefficients of luminous intensity R' for sample 4 at observation angle α (0.2° , 0.33° , 1° , 1.5°) and illumination angles β_1 and β_2 : a): $\beta_1 = 0^\circ$ and $\beta_2 = 0^\circ$, $\beta_2 = 5^\circ$, $\beta_2 = 10^\circ$, $\beta_2 = 15^\circ$, $\beta_2 = 10^\circ$, $\beta_2 = 20^\circ$, $\beta_2 = 30^\circ$; b): $\beta_2 = 0^\circ$ and $\beta_1 = 0^\circ$, $\beta_1 = 5^\circ$, $\beta_1 = 10^\circ$, $\beta_1 = 15^\circ$, $\beta_1 = 10^\circ$, $\beta_1 = 20^\circ$, $\beta_1 = 30^\circ$.

As can be seen from **Figures 8-11**, the coefficient of luminous intensity (R') depends on three measurement geometry. A comparison of test results for illumination angles β_1 and β_2 and for the observation angles adopted (0.2° , 0.33° , 1° , 1.5°) revealed that at illumination angles of 0° - 15° the value of R' is constant for

samples 1 and 2 (reflective textile tapes), reaching a maximum at an illumination angle of 20° , and then decreasing.

Comparing the photometric properties of samples 1 and 2 (textile tapes), it should be noted that the R' coefficient for sample 1 is lower by 6.5%, which is

attributable to the morphological structure of the tape (**Figure 2**). A higher R' was found for sample 2, in which the microlenses have smaller diameters. In addition, in the case of reflective textile materials, photometric properties change for varying angles of illumination. For sample 1, this change amounts

to as much as 15% (as compared to almost 6% for sample 2).

In the case of highly reflective microprismatic polymer films, R' reaches a maximum at an illumination angle of 0° , and then progressively decreases with increasing illumination angles. The maximum R' value is $490 \text{ cd} \cdot \text{lx}^{-1} \cdot \text{m}^{-2}$ for retroreflective microlens materials (samples 1 and 2, **Figures 8** and **9**) and $659 \text{ cd} \cdot \text{lx}^{-1} \cdot \text{m}^{-2}$ for microprism materials (sample 4, **Figure 11**). Sample 3 shows the lowest reflective properties (see **Figure 10**), which should be attributed to the negative effect of its color (red) [21, 22].

In addition, for all reflective materials analysed, the best reflective properties (maximum R' coefficient) were found at observation angles of 0.2° and 0.33° . For observation angles of 1° and 1.5° , the R' values for all samples tested assume significantly lower values. The estimated percentage changes in the R' coefficient in dependence on the observation angle are presented in **Tables 2** and **3**.

The results show that a change in the observation angle α from 0.2° to 0.33° leads to relative changes in the relative R' ranging from 17.44% to 29.56%, whereas a change in the observation angle from 0.2° to 1.5° results in a reduction in the relative R' ranging from 88.68% to 97.14%. This is true of all the samples tested, regardless of the base material and retroreflective technology.

For the samples analysed, changes in the coefficient of luminous intensity R' are also affected by illumination angles in the range 0° - 30° (**Table 4**).

Percentage changes in the R' coefficient are significantly smaller for reflective materials with microlenses applied on a textile base (1.75-22.29%) in comparison to microprism materials (31.35-52.8%). It could be assumed that microprism technology is more sensitive to changes in observation geometry, and that the reflective properties of these products decrease faster than those of microlens materials.

Summary

In conclusion, the optical properties of retroreflective materials depend on the observation and illumination angles. As can be seen from **Figures 8-11**, the luminous intensity coefficient (R') depends on the technology used in the production

Table 2. Relative changes in the coefficient of luminous intensity R' between $\alpha = 0.2^\circ$ and $\alpha = 0.33^\circ$. Note: The relative change in R' was calculated from the following formula: $\Delta R' = [(R'(\alpha = 0.2^\circ) - R'(\alpha = 0.33^\circ)) / R'(\alpha = 0.2^\circ)] \cdot 100\%$.

Entrance angles (β_1, β_2)	Relative change in R' $\Delta R', \%$			
	Sample 1	Sample 2	Sample 3	Sample 4
$\beta_1 = 0^\circ, \beta_2 = 0^\circ$	30.00	26.97	29.23	13.84
$\beta_1 = 0^\circ, \beta_2 = 5^\circ$	29.65	27.33	29.4	13.96
$\beta_1 = 0^\circ, \beta_2 = 10^\circ$	29.23	27.74	29.27	14.09
$\beta_1 = 0^\circ, \beta_2 = 15^\circ$	29.33	27.67	28.74	14.47
$\beta_1 = 0^\circ, \beta_2 = 20^\circ$	29.40	26.65	28.57	17.76
$\beta_1 = 0^\circ, \beta_2 = 25^\circ$	29.77	24.17	29.68	21.22
$\beta_1 = 0^\circ, \beta_2 = 30^\circ$	29.55	20.81	28.25	26.74
$\beta_1 = 5^\circ, \beta_2 = 0^\circ$	30.36	26.49	29.41	13.85
$\beta_1 = 10^\circ, \beta_2 = 0^\circ$	31.12	26.91	29.41	12.88
$\beta_1 = 15^\circ, \beta_2 = 0^\circ$	32.62	26.74	27.21	10.62
$\beta_1 = 20^\circ, \beta_2 = 0^\circ$	33.94	26.73	25.62	14.32
$\beta_1 = 25^\circ, \beta_2 = 0^\circ$	33.36	23.69	23.92	14.92
$\beta_1 = 30^\circ, \beta_2 = 0^\circ$	24.61	24.61	22.57	13.53
Mean	30.23	25.89	27.80	15.55

Table 3. Relative changes in the coefficient of luminous intensity R' between $\alpha = 0.2^\circ$ and $\alpha = 1.5^\circ$. Note: Relative changes in R' were calculated from the following formula: $\Delta R' = [(R'(\alpha = 0.2^\circ) - R'(\alpha = 1.5^\circ)) / R'(\alpha = 0.2^\circ)] \cdot 100\%$.

Entrance angles (β_1, β_2)	Relative change in R' $\Delta R', \%$			
	Sample 1	Sample 2	Sample 3	Sample 4
$\beta_1 = 0^\circ, \beta_2 = 0^\circ$	96.16	89.52	96.15	96.95
$\beta_1 = 0^\circ, \beta_2 = 5^\circ$	96.30	89.56	98.00	96.70
$\beta_1 = 0^\circ, \beta_2 = 10^\circ$	96.45	89.59	97.86	96.89
$\beta_1 = 0^\circ, \beta_2 = 15^\circ$	96.38	89.43	97.66	96.88
$\beta_1 = 0^\circ, \beta_2 = 20^\circ$	95.91	88.91	97.34	96.71
$\beta_1 = 0^\circ, \beta_2 = 25^\circ$	94.83	87.64	96.78	96.82
$\beta_1 = 0^\circ, \beta_2 = 30^\circ$	94.24	86.10	96.19	97.08
$\beta_1 = 5^\circ, \beta_2 = 0^\circ$	96.25	94.72	97.84	96.70
$\beta_1 = 10^\circ, \beta_2 = 0^\circ$	96.30	94.86	97.48	96.89
$\beta_1 = 15^\circ, \beta_2 = 0^\circ$	96.71	95.07	96.99	96.88
$\beta_1 = 20^\circ, \beta_2 = 0^\circ$	97.32	95.13	96.91	96.71
$\beta_1 = 25^\circ, \beta_2 = 0^\circ$	96.91	94.42	97.12	96.82
$\beta_1 = 30^\circ, \beta_2 = 0^\circ$	95.77	93.57	97.05	97.08
Mean	96.12	91.42	97.18	96.85

Table 4. Percent change in R' in dependence on changes in illumination angles β_1 and β_2 .

Sample No.	Average % changes in R' from $\beta_1 = 0^\circ$ to $\beta_1 = 30^\circ$	Average % change in R' from $\beta_2 = 0^\circ$ to $\beta_2 = 30^\circ$
	$\Delta R'$	$\Delta R'$
1	1.75	12.86
2	12.74	22.29
3	44.51	31.35
4	52.08	50.80

of retroreflective products. Analysis of the maximum values of the luminous intensity coefficient shows that reflective microprism materials (polymer foils) have more favourable reflective properties, affording higher R' coefficients.

Materials containing a textile base behave differently from polymeric tapes. The fabric structure clearly leads to the

heterogeneous aggregation of microlenses, which has a direct adverse effect on their photometric properties. The R' coefficient of woven fabrics is lower than that of reflective polymer foils by up to $169 \text{ cd} \cdot \text{lx}^{-1} \cdot \text{m}^{-2}$, or by over 25% (excluding sample 3). However, in terms of the stability of reflective properties under conditions of varying observation angles, microlens technology appears to be superior.

The findings indicate that in choosing reflective materials the colour is also of the essence as it affects their photometric properties, with light colours being preferable. In practice, due to the directional reflection of light by retroreflective materials, the user's safety depends on the ambient conditions, the angle of illumination by vehicle headlights, and the type of reflective material (reflective layer technology, substrate type, and colour). When retroreflectors are oriented at an angle of $\pm 2^\circ$ between a line perpendicular to the surface of the retroreflector and the incident light beam (e.g., the vehicle headlights), the luminous intensity coefficient R' decreases by more than 50 times (especially in the case of microprisms) in comparison to an observation angle of $\alpha = 0.2^\circ$.

Materials containing microprisms exhibit higher luminous intensity than reflective microlens tapes for illumination angles up to 15° . However, at illumination angles greater than 15° , reflective microprism materials are characterised by a faster decrease in R' values (in relation to microlens tapes). This phenomenon is caused by the greater dispersion of light reflected by microlenses compared to microprisms due to the less regular orientation of microlenses and the lower homogeneity of textile fabrics vs. polymer foils. Materials containing microprisms offer more efficient directional reflection of light (at low observation and illumination angles), which enhances the visibility of people moving along a road parallel to the direction of moving vehicles outside residential zones. On the other hand, in materials containing microlenses, the R' coefficient is less dependent on the illumination and observation angles, and thus they afford superior visibility on a road at greater angles in relation to the direction of oncoming vehicles. This

phenomenon is of particular importance for the safety of people wearing reflective materials in residential areas, e.g., when approaching pedestrian crossings. Pedestrians using microlens accessories may be more easily noticed by drivers before stepping onto a road. In addition, the reflection coefficient depends on the surface of the material (see Formula 1). In order to ensure good visibility of users, it is necessary to equip them with several reflective elements, preferably arranged uniformly around the body.



Acknowledgements

This paper is based on the results of a research task carried out within the scope of the third phase of the National Program "Improvement of occupational safety and working conditions," co-financed in the years 2014-2016 in the area of tasks related to services for the state by the Ministry of Labour and Social Policy. The program coordinator was the Central Institute for Labour Protection – National Research Institute (CIOP-PIB).

References

- Road accidents in Poland in 2017; Police Headquarter; Warsaw, 2018.
- Road Traffic Law. The Act of June 20, 1997. *Journal of Law* 1997; 98, 602.
- Report on the results of inspection of high visibility reflective accessories; Office of Competition and Consumer Protection (UOKiK); Warsaw 2015.
- Information materials of SATRA Technology „High-visibility retro-reflective materials” <https://www.satrapl.com/spotlight/article.php?id=343>; available 20.02.2019.
- 3M brochure; “Scotchlite Reflective Material Visibility Solutions”, <http://multimedia.3m.com/mws/media/7656940/3m-visibility-solutions-brochure.pdf>; available 20.02.2019
- William P. Rowland. US Patent 3,689,346; 1972.
- Hoopman. US Patent 4,588,258; 1986.
- Szczech. US Patent 5,138,488; 1992.
- Wilsen. US Patent 5,780,140; 1998.
- EN 13356:2001. Visibility accessories for non-professional use. Test methods and requirements.
- Matusiak M, Kosiuk G. Clothing accessories improving a visibility on the road. *Technologia i Jakość Wzrostów* 2017; 62: 113-126.
- Nycz E i in. Budowa tkanin. WSIP; W-wa 1990. ISBN 83-02-03229-8.
- Jackowski T, Szosland J, Korliński W. *Podstawy mechanicznej technologii tekstyliów*.
- WNT; Warszawa 1987.
- Szosland J. *Struktury tkaninowe*. Łódź 2007. ISBN 83-86492-42-2
- Cieślak M. O tym do czego służą odblaski. *Foton* 2009; 107: 23-31. Instytut Fizyki, Uniwersytet Jagielloński.
- Hua H, Gao CM, Rolland J P. Study of the Imaging Properties of Retro-reflective Materials Used in Head-Mounted Projective Displays (HMPDs). *Proceedings of SPIE*, Vol. 4711; ISSN 0277-786X; 2002.
- Costa M, Bonetti L, Bellelli M, Lantieri C, Vignali V, Simone A. Reflective Tape Applied to Bicycle Frame and Conspicuity Enhancement at Night. *Human Factors* 2017; 59, 3: 485-500. <http://dx.doi.org/10.1177/0018720816677145>.
- Durability test of retro-reflecting materials for road signs at Nordic test sites. *Traffic Engineering & Control* 2005; 46, 1: 13-7. <http://worldcat.org/issn/00410683>.
- Intersection Proven Safety Countermeasure: Technical Summary: Backplates with Retroreflective Borders 2015; 16p. http://safety.fhwa.dot.gov/intersection/blackplates/blackplate_tech/sa15007.pdf; available 20.02.2019.
- CIE 1982; No 54 Retroreflection. Definition and measurement.
- <http://reflectivetape.info/514-2/>; available 20.02.2019.
- <https://blog.signwarehouse.com/a-basic-guide-to-reflective-vinyl/>; available 20.02.2019.

Received 08.01.2019 Reviewed 27.02.2019

